S. S. Rogers[1]
P. Venema[2]
J. P. M. van der Ploeg[3]
E. van der Linden[2]
L. M. C. Sagis[2]
A. M. Donald[1]
[1] *Cambridge University, Department of Physics, Cavendish Laboratory, Cambridge, CB3 0HE, UK*

[2] *Wageningen University, Laboratory of Food Physics, P. O. Box 8129, 6700 EV Wageningen, The Netherlands*

[3] *Leiden University, Institute of Chemistry, P. O. Box 9502, 2300 RA Leiden, The Netherlands*

Investigating the Permanent Electric Dipole Moment of β-Lactoglobulin Fibrils, Using Transient Electric Birefringence

Received 27 September 2005; revised 25 January 2006; accepted 6 February 2006
Published online 17 February 2006 in Wiley InterScience (www.interscience.wiley.com). DOI 10.1002/bip.20483

Abstract: *Amyloid fibrils, which are polymeric assemblies of protein molecules, have been intensively studied on a structural level, yet due to complications such as the disorder within the molecules, several aspects of their structure remain mysterious. Similarly, the kinetics of assembly are not well understood. Here we investigate the electric dipole moment of* β*-lactoglobulin fibrils, a model amyloid fibril system, by applying the technique of transient electric birefringence. This moment appears to be large, and comparable to the total moment of the constituent protein monomers if they were joined in a chain, head-to-tail, without changing conformation, suggesting an ordered joining of monomers in the fibril. Such an ordered assembly may have implications for the assembly mechanism of* β*-lactoglobulin fibrils in particular, and amyloid fibrils in general.*

This article was originally published online as an accepted preprint. The "Published Online" date corresponds to the preprint version. You can request a copy of the preprint by emailing the Biopolymers editorial office at biopolymers@wiley.com

Keywords: *amyloid; dipole; electric; birefringence; lactoglobulin*

Correspondence to: E. van der Linden (e-mail: erik.vanderlinden@wur.nl) or A. M. Donald (e-mail: amd3@cam.ac.uk)
Contract grant sponsor: BBSRC and European Commission, Improving Human Potential programme.

INTRODUCTION

Several proteins have the ability to self-assemble into rod-like structures, known as amyloid fibrils, in mildly denaturing conditions.[1–4] These fibrils occur in vivo in several human diseases,[1–4] but they can also be formed in vitro from a wide range of proteins, including many not associated with any disease.[3,4] Nowadays, amyloid fibrils are usually defined in terms of their common structural characteristics, apparently caused by generic features of a polypeptide chain.[3–7] The main defining characteristic of amyloid fibrils is the *cross-β* structural motif, in which intermolecular β-sheets extend over the length of the fibril, such that each β-strand runs perpendicular to the fibril axis. This motif, which was originally revealed by X-ray fiber diffraction,[5] is held together by hydrogen bonding between atoms of the polypeptide backbones, and so is largely independent of the primary structure of the protein or peptide from which the fibril forms.[2,3]

In recent years, more detailed structural information on amyloid fibrils has been obtained (reviewed in Ref. 6). Solid-state nuclear magnetic resonance (NMR) methods have proven particularly valuable for determining structural constraints in fibrils composed of short peptides. Detailed structural models have thus been proposed for peptide fragments of transthyretin $TTR_{105–115}$ (Ref. 8) and β-amyloid peptide $A\beta_{1–40}$.[9,10] These and other NMR studies confirm that the residues involved in the cross-β motif are well ordered, in terms of both conformation and the registry of intermolecular hydrogen bonds. Moreover, the recently determined crystal structure of a 7-residue peptide fragment of the yeast prion Sup35 (Ref. 11) shows that this peptide assumes a similarly well-ordered cross-β conformation in solution conditions close to those in which it forms fibrils. Nevertheless, there is a lack of detailed structural information on fibrils formed from larger proteins. Just as the folding of large proteins into their native states tend to be more hindered by metastable, intermediate, and misfolded states than the folding of small proteins,[12] we may wonder whether larger proteins could form amyloid fibrils, in which the proteins can assume multiple alternative conformations, even though amyloid fibrils formed from small proteins tend to assume a single well-ordered conformation.

β-Lactoglobulin solutions form fibrils under prolonged heating at low pH and low ionic strength. Investigation of these fibrils shows that they may be classified as amyloid fibrils: their X-ray fiber diffraction pattern is indicative of the cross-β motif; they bind the amyloid-specific dyes, Thioflavin T and Congo red; and they show increased β-sheet content relative to their native state.[13,14] These fibrils are polydisperse in length (with typical lengths of the order of 1 μm) and monodisperse in cross-section, with a diameter of about 4 nm.[15,16] The persistence length has been estimated as approximately 1.6 μm—of the same order of magnitude as the length.[17] Using atomic force microscopy (AFM), the fibrils show a twisted strand structure with a repeat distance of 26 nm,[16] one or two protein monomers across in cross-section.[14–16,18] The line density of molecules in the fibril (monomers per unit length), determined by neutron scattering measurements, is 0.28 nm^{-1}, which approximately equals the inverse of the monomer's diameter.[15] It seems therefore that each fibril is composed of a single chain of monomers or "protofilament."[14] The fibrils are highly charged at low pH with an ionic charge of around $+21e$ per monomer at pH 2.[15,19] Under conditions of pH 2, 5 mg/mL protein concentration, no added salt and incubation at 80°C, transparent solutions of fibrils are produced with very few spherulites.[15,17] In previous articles, we studied this system's length distribution using flow birefringence[20] and electric birefringence relaxation.[21] As a model amyloid fibril system, β-lactoglobulin fibrils have some interesting characteristics. The simplicity of their cross-sectional structure is in contrast with many other fibril systems where complex arrangements of filaments are observed, and they are composed of a complete protein rather than a short peptide sequence.

The technique of transient electric birefringence (TEB) was originally developed by Benoît[22] and O'Konski and Zimm,[23] and probes the electric and diffusive properties of particles in solution. Pulses of an electric field are applied to the solution, and the resulting alignment of the particles causes birefringence or dichroism in the solution, which can be measured with polarized light. For anisotropic particles such as rods or fibrils, the behavior of the particles in an electric field depends on three physical characteristics: their rotational diffusivity, electric polarizability, and permanent dipole moment.* The theory of Benoît quantitatively describes the dynamics of particles in the field, assuming the particles to be rigid and uniaxial. TEB has also been used to address other diverse problems in structural biology.[25]

* As highlighted by Felder et al.,[24] the formally defined concept of a dipole moment does not apply to a particle with a net charge, and we ought rather to talk about the first moment of the charge distribution around its rotational center of drag. However, because authors generally call this the dipole moment, and because it is most easily visualized as such, we will call it the dipole moment in this article.

In our previous study,[21] TEB was performed on a solution of β-lactoglobulin fibrils, and the electric field pulses was purposefully made as short as possible to minimize the effect due to the permanent electric dipole moment of the fibrils. The measurements were consistently described using Benoît's model,[22] where the polarizability has a magnitude given by Fixman's theory.[26]

In this article, we describe other TEB experiments that were performed on the same fibril solution, but with the specific objective of examining the permanent electric dipole moment. However, what appears to be a permanent dipole moment may not be *permanent*, but may comprise, wholly or partly, an induced dipole moment that is *slow* to relax. Therefore we will assess the ambiguity due to slow polarization. Measurements of the permanent electric dipole moment of β-lactoglobulin or other amyloid fibrils may have interesting implications for the structure and formation of amyloid fibrils in general.

THEORETICAL BACKGROUND

Dynamics of Rigid Rods in a Transient Electric Field

In this section, we describe the interpretation of transient electric birefringence of anisotropic particles, in terms of their orientation and relaxation, as developed by Benoît.[22] This model will be used to analyze our TEB measurements of β-lactoglobulin fibrils below.

The orientational distribution $f(\mathbf{u}, L, t)$, of rigid uniaxial particles of length L, having a rotational diffusivity $D_r(L)$ and oriented in the direction $\mathbf{u}$ obeys the equation of motion:[22]

$$\nabla^2 f + \frac{1}{k_B T}\nabla \cdot (f \nabla w) = \frac{1}{D_r}\frac{\partial f}{\partial t}, \qquad (1)$$

where w is the potential energy of the particle in the field and t is time. If spherical polar coordinates (θ, φ) are set up so that the electric field E is in the direction $\theta = 0$, then

$$\nabla w = -(\Delta\alpha E^2 \cos\theta - \mu E)\sin\theta \mathbf{e}_\theta, \qquad (2)$$

where $\Delta\alpha(L)$ and $\mu(L)$ are the anisotropy of polarizability and the permanent dipole moment of the particle, respectively, and $\mathbf{e}_\theta$ is the unit vector in the θ direction. The problem is thus rotationally symmetric in φ, and $f(\mathbf{u}, L, t)$ can be replaced with $f'(\theta, L, t)$.

For light propagating perpendicular to the field, the birefringence Δn is given by

$$\Delta n = M \int_0^\infty c_L(L) S(L) \mathrm{d}L, \qquad (3)$$

where M is the optical anisotropy per unit length concentration $c_L(L)S(L)dL$, and $S(L)$ is the alignment parameter of the fibrils with length L, defined as

$$S(L,t) \equiv \int_0^\pi P_2(\theta) f'(\theta, L, t) \sin\theta \mathrm{d}\theta \qquad (4)$$

where $P_2(\theta) = (3\cos^2\theta - 1)/2$, the second Legendre polynomial.

In Benoît's model, the induced polarization of the particles occurs instantaneously, as implicit in taking $\Delta\alpha(L)$ to be constant with respect to time. Making this assumption of instantaneous polarization, Eqs. (1)–(4) can be used to calculate the initial rise gradient of the birefringence $\Delta\dot{n}_{\mathrm{init}}$, if the field is switched on at $t = 0$, i.e., the field strength is zero at $t < 0$, and E at $t \geq 0$. As calculated in Ref. 21, a prediction of $\Delta\dot{n}_{\mathrm{init}} \propto E^2$ is obtained, reminiscent of the Kerr law, though it applies to the initial rise of birefringence rather than the steady state at long times.

However, the induced polarization of real particles may not be instantaneous. If the polarization relaxes with some characteristic time, then the polarizability of the fibrils will be zero at $t = 0$, so $\Delta\dot{n}_{\mathrm{init}} = 0$ also. The rise of the birefringence will be delayed by the relaxation time of the polarizability.

Diffusivity of Rods

For rod-like particles in the dilute regime, the rotational diffusion coefficients D_r has been studied by Riseman and Kirkwood,[27] Broersma,[28] and Tirado and Garcia de la Torre.[29] All three studies give D_r, which can be written in the form:

$$D_r = \frac{3k_B T(\ln(L/d) - \gamma)}{\pi\eta L^3}, \qquad (5)$$

where k_B is Boltzmann's constant, T is the absolute temperature, L is the rod length and d its diameter, η is the viscosity of the solvent, and γ is a numerical correction factor that differs between the treatments. Broersma[28] calculated γ for long cylinders:

$$\gamma = 0.887 - 7\left[\frac{1}{\ln(L/d)} - 0.28\right]^2, \qquad (6)$$

and showed that this expression gave accurate values of D_r for aspect ratios $L/d \gtrsim 5$. Rotational diffusiv-

ities of the form of Eq. (5) have been experimentally verified for many systems of stiff polymers in dilute solution, (see, e.g., Ref. 30). In Eq. (5), D_r has a significant dependence on L and a slight dependence on d.

Polarizability of Polyelectrolyte Rods

In our previous study,[21] we found that Fixman's theory of the polarizability of polyelectrolyte rods[26] gave a reasonable prediction of $\Delta\alpha$ for β-lactoglobulin fibrils. Fixman predicted[26]

$$\Delta\alpha = \frac{4\pi\varepsilon\varepsilon_0 LKz_1}{\gamma^2(z_1 - z_2)}\left(1 - \frac{\tanh(\gamma L/2)}{\gamma L/2}\right), \qquad (7)$$

where z_1 and z_2 are the valencies of the counter- and coions, and the relative permittivity of water, $\varepsilon = 80.1$. The γ^{-1} is the characteristic "screening length" given by

$$\gamma^2 = \frac{4\pi c_1 Kb}{\phi}, \qquad (8)$$

where c_1 is the bulk concentration of counterions, b is the mean spacing of charges on the polyion, and K is a numerical factor given by

$$K = [2\ln(2L/d) - 14/3]^{-1}, \qquad (9)$$

where d is the diameter of the cylinder. The fraction of bound counterions, φ, is given by the Manning condensation theory:[31]

$$\phi = 1 - \frac{b}{Q}, \qquad (10)$$

where $Q = e^2/4\pi\varepsilon\varepsilon_0 k_B T$ is the Bjerrum length.

According to Eq. (7), $\Delta\alpha$ has an L^3 dependence at small L, which gradually changes to a linear L dependence at large L.

Several authors[32–34] consider the Fixman theory to be the most useful model of rod-like polyelectrolyte electric polarization. Other models have been published, based on similar physics and reaching similar results, and applying to particles with various geometries. Most are discussed in Ref. 32 or stem from work reviewed therein.

The Fixman theory has also been compared with experimental results for DNA fragments by Elias and Eden[30] and polystyrene–sulfonate chains by Tricot and Houssier.[35] Both studies used samples that were nearly monodisperse, allowing polarizability to be measured at a range of lengths. Elias and Eden confirm an L^3 dependence of polarizability at small L, which decreases to an approximately linear dependence at large L. Tricot and Houssier again found a dependence close to L^3 at small L, decreasing to a much smaller dependence at large L. The absolute values predicted by the Fixman theory was found to give useful, though not accurate, values approximately within a factor of 2 of the experimental results.

The relaxation behavior of the polyelectrolyte polarizability is also not well understood. In the theories of double-layer polarization, the relaxation is governed by the motion of small ions along the full length of the polyelectrolyte.[32] The characteristic relaxation time $\tau_{\Delta\alpha}$ is therefore of the order

$$\tau_{\Delta\alpha} \sim L^2\zeta/k_B T, \qquad (11)$$

where ζ is the friction coefficient of small ions. We may calculate a quick estimate of this time for polyelectrolyte rods of length 1 μm, surrounded by freely diffusing counterions of hydrodynamic diameter $\sim$5 Å. Using the Stokes drag to calculate ζ, we obtain a relaxation time of $\sim$2 ms. However, van Dijk et al.,[36] who obtained a polarizability almost identical to Eq. 7, predicted that ion flux out of the double layer dominates the relaxation for $L \gg \gamma^{-1}$. For long rods, $\tau_{\Delta\alpha}$ is therefore fixed at a much smaller value, independent of length:

$$\tau_{\Delta\alpha} \sim \zeta/k_B T\gamma^2. \qquad (12)$$

A review of experimental results shows that the situation is more complicated than these theories predict. There are at least two relaxation processes of polarized polyelectrolytes.[37] A fast mode occurs on typical time scales of $-$10 ns to 1 μs, which is dependent on counterion concentration, qualitatively following Eq. (12), but a slow mode occurs on typical times scales $\sim$1 ms, which is independent of counterion concentration.[37] The fast and slow relaxation modes may correspond to the movement of free ions and bound ions respectively.[37]

In our previous study, we found that our β-lactoglobulin fibril solutions obeyed the predicted relationship between the initial rise gradient of the birefringence, and the field strength, assuming instantaneous induced polarization; $\Delta\dot{n}_{\text{init}} \propto E^2$,[21] where the gradients were measured on a time scale $\sim$1 μs. Using Fixman's prediction for the magnitude of the induced polarization, and treating this polarization as instantaneous, we found that the birefringence response from 240 μs pulses led to a prediction of the length distribution of the fibrils, in reasonable agreement with the results of our earlier flow birefringence technique.[20] However, these results do not preclude the existence

of additional slower components of the polarizability, provided that if slower components exist, their relaxation times are much greater than the pulse time of 240 μs, or that they have a much smaller contribution than $\Delta\alpha$ according to Fixman.

Because of the previous results, it is reasonable to model the induced polarization of the fibrils as instantaneous, with a magnitude given by Fixman's theory. However, we must be aware of the possibility of additional components of slow polarization of the fibrils and assess their effect on the results.

MATERIALS AND METHODS

β-Lactoglobulin Fibril Preparation

All experiments were performed on bovine β-lactoglobulin obtained from Sigma (Gillingham, UK) (L-0130-5G, batch 033K7003, a mixture of genetic variants A and B). The protein was dissolved in dilute hydrochloric acid at pH 2, and extensively dialyzed with the same pH 2 hydrochloric acid to remove traces of calcium ions and obtain a solution with the same ionic strength as the solvent. The solution was centrifuged at 22600 g for 30 min and filtered through a 0.45-μm filter to remove aggregates and undissolved protein. An ultraviolet (UV) spectrophotometer was used to measure the concentration of this stock solution, using a calibration curve from known β-lactoglobulin concentrations, determined at a wavelength of 278 nm. The stock solution was used to make a 15-mL sample that was made up to 5 mg/mL protein concentration, in pH 2 HCl with no added salt. It was heated in a glass vessel for 24 h at 80°C using a water bath, during which it was stirred constantly with a magnetic stirrer. Sodium azide (200 ppm) was added to the resulting fibril solution to prohibit microbial growth, and the solution refrigerated at 4°C before measurements were made. This preparation is identical to that used previously for our rheo-optics study.[20] The measurements presented here and in our previous article[21] were made on the same sample.

Electro-Optical Experiments

A conventional polarimeter, based on crossed polarizers with an adjustable quarter-wave plate, was used to measure electric birefringence (as described fully in Ref. 38). Light from an 8 mW helium–neon laser (632.8-nm wavelength) first passes through a high-quality Glan–Thompson polarizer, followed by a cell containing the solution, across which the electric field is applied. Next it passes through a quarter-wave plate at an adjustable angle, followed by a second Glan–Thompson polarizer. Finally, its intensity is measured using a photomultiplier tube. The presence of the quarter-wave plate allows positive and negative birefringence to be distinguished, and improves the sensitivity. (This setup is also described in Ref. 21).

The voltage of the photomultiplier tube and the voltage applied on the solution are measured simultaneously by a digital oscilloscope (LeCroy 9450). The voltage of the tube is calibrated to obtain the birefringence signal. The solution is contained in a quartz cuvette with two parallel, rectangular platinum electrodes. The electrodes are held apart at a fixed distance of 1.89 mm, and the optical path length is 49.05 mm, the length of the electrodes. The temperature is kept constant at 21°C by circulating water from a thermostated bath through a jacket which holds the cell. The voltage to be applied across the electrodes is supplied by a function generator (WaveTek 29) in combination with a high-speed power amplifier (NF Electronic Instruments 4020, bandwidth 500 KHz, max 250 V). The voltage response time of the setup is better than 1 μs.

The sample was subjected to transient pulses of an electric field, and the birefringence response measured. In order to reduce the noise, responses from repeated, identical pulses were collected and averaged, leaving a lag time between them for the system to equilibrate. This lag time was judged long enough when the optical response to successive pulses stayed the same, within the noise of measurement. Each measurement presented here is the mean response from 32 identical, successive pulses, with a lag time of 60 s. The fibril solution, as prepared above, was diluted 100 times in low concentration HCl so that it had a final HCl concentration of 0.2 m*M*.

Experiments were performed on the same β-lactoglobulin fibril solution as measured in our previous study.[21] The prepared solution was diluted 100 times in low concentration HCl so that it had a final HCl concentration of 0.2 m*M*. The ionic conditions of the diluted sample were therefore also identical to those of the previously analyzed results.

Numerical Method

The numerical calculations described in this article were implemented using Matlab's built-in partial differential equation solver (The Mathworks, Natick, MA, USA), which uses a Runge–Kutta method. Care was taken to ensure that the resolutions of time and angle were high enough, so that numerical error could be neglected.

RESULTS

A solution of β-lactoglobulin fibrils was prepared, diluted, and subjected to pulsed electric fields as described above. Under a single, steady 10-ms pulse at a field strength of 54 kV m^{-1}, the birefringence can be seen to rise steadily from zero during the pulse, as shown in Figure 1. The birefringence is caused by the alignment of the fibrils, and does not reach a steady state during the pulse, because the time is short compared to the rotational diffusion time of the fibrils, as seen in our previous study.[21] At the end of the pulse, the birefringence decays slowly to zero,

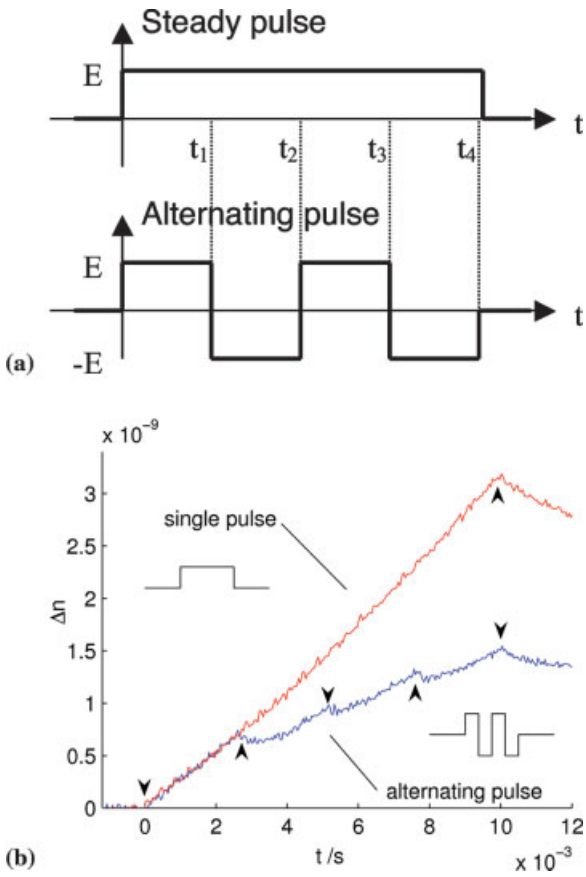

FIGURE 1 (a) Steady and alternating electric fields. The t_2 is the time of the second field reversal. (b) Birefringence measurements from a solution of β-lactoglobulin fibrils in a pulsed electric field. Under a single, steady pulse, the birefringence increases monotonically during the pulse, but under an alternating pulse, the birefringence exhibits a cusp at each field reversal, indicative of a permanent or slowly relaxing electric dipole moment. (Arrows indicate points at which field is applied, reversed, and removed.)

as the alignment of the fibrils is lost by rotational diffusion.

If, instead of a single steady pulse, pulses of alternating polarity are applied to the solution, a new feature is seen. We applied an "alternating pulse," i.e., 4 pulses of alternating polarity, each of duration 2.5 ms, to the sample. At every reversal of the field, the birefringence $\Delta n(t)$, exhibits a cusp, decreasing before increasing again (Figure 1). Cusps like these can be caused if the fibrils possess a nonzero permanent electric dipole moment, which is aligned along the fibril axis.[22] (More precisely, the angle between the permanent dipole moment and the fibril axis ψ, must be less than $\tan^{-1}\sqrt{2} = 54.7^\circ$ to produce cusps like these. If $\psi > 54.7^\circ$, the gradient of Δn would *increase* upon field reversal[39]).

The cusps may be interpreted qualitatively as follows. During the initial pulse, the fibrils begin to rotate toward alignment in the direction of the field. The field is externally controlled and can be reversed within 1 μs. When the field is reversed, the permanent dipole moment is left opposing the field because it is fixed relative to the fibril axis. The reversal therefore puts an opposing torque on the fibril, rotating it in the opposite direction and reducing its alignment, causing the birefringence to drop. In Figure 1(b), this drop due to the field reversal is significant compared to the steady increase of birefringence under the steady pulse, suggesting that the permanent dipole moment has a comparable magnitude to the induced moment.

However, within this interpretation, the permanent dipole moment may not be *permanent*, but merely *slow* to relax. In this case, the induced moment would be left opposing the field after the reversal, just like a true permanent moment. If the rotational diffusion is comparable to, or faster than, the relaxation of the induced moment, then the dipoles will relax by reorientation after the field reversal, again producing cusps in the birefringence.

As discussed above, our previous results were successfully modeled by assuming only a fast component of the polarizability, with a relaxation time 1 μs and a magnitude given by Fixman's theory.[26] However, this observation does not preclude the existence of a slow component of the polarizability, provided that its relaxation time is much greater than the pulse time of 240 μs, or that it has a small magnitude compared to the fast component.

Because no slow polarizability component was observed previously, we will start by neglecting it. A permanent dipole moment of the fibrils can then be obtained from the results, but we must be aware that it may contain a contribution that is not *permanent* but merely *slow*. The possible contribution of slow polarization will be assessed in the Discussion.

ANALYSIS

Based on the measurements of Figure 1(b), and neglecting any slow component of polarizability, we can calculate the permanent dipole moment of the fibrils in two ways. First, we present a quick and direct estimate, based on analytical approximations. Second, we present a more detailed analysis, based on a numerical calculation of the birefringence, where we use the fibril length distribution as determined for the same sample in Ref. 21. In order to use Benoît's model,[22] we assume the permanent dipole

moment is aligned with the fibril axis ($\psi = 0$), and shall discuss this assumption subsequently.

Estimating the Dipole Moment Analytically

An estimate of the dipole moment can be made by analyzing the system in a simplified way. Instead of considering the full distribution of lengths, we consider a monodisperse system of fibrils of length L_τ: the length of a fibril that would have a rotational diffusion time equal to the mean decay time of the birefringence, τ. (L_τ can be thought of as the mean length of fibrils weighted by their relative alignment in the field.) Each fibril of length L_τ has a permanent dipole moment of magnitude $\mu(L_\tau)$ that we wish to estimate and an anisotropy of electric polarizability $\Delta\alpha(L_\tau)$ that can be calculated using Fixman's theory for polyelectrolyte rods, described above.

The evolution of the orientational distribution $f'(\theta, t)$ in time depends on the polarizability $\Delta\alpha$, rotational diffusivity D_r, and permanent dipole moment of magnitude μ, directed parallel to the rod axis. As Benoît showed,[22] the transient electric birefringence in weak fields can be described analytically by expanding $f'(\theta, t)$ in terms of Legendre polynomials:

$$f'(\theta, t) = \frac{1}{2}\sum_n a_n(t) P_n(\cos\theta) \tag{13}$$

In the electric field, the coefficients $a_n(t)$ are described by the coupled differential equations

$$\begin{aligned}
&\frac{1}{D_r}\frac{da_0}{dt} = 0,\\
&\frac{1}{D_r}\frac{da_1}{dt} = 2pa_0 - 2a_1\left(1 - \frac{1}{5}q\right) - \frac{2}{5}pa_2 - \frac{6}{35}qa_3,\\
&\frac{1}{D_r}\frac{da_2}{dt} = 2qa_0 + 2pa_1 - 2a_2\left(3 - \frac{1}{7}q\right) - \frac{6}{7}pa_3 - \frac{8}{21}qa_4,
\end{aligned} \tag{14}$$

where

$$\begin{aligned}
p &= \frac{\mu E}{k_B T},\\
q &= \frac{\Delta\alpha E^2}{k_B T}.
\end{aligned} \tag{15}$$

If the electric field strength E is low, such that p and q are small, the following approximation can be made: only coefficients a_0, a_1, and a_2 are non-negligible, and Eqs. (14) then have the general solution,

$$\begin{aligned}
a_0 &= 1,\\
a_1 &= p\left[1 + \frac{2}{15}q - \frac{1}{15}p^2 + \left(2 + \frac{2}{35}q - \frac{1}{10}p^2\right)\right.\\
&\qquad \left. \times \frac{A}{p^2}e^{-r_1 D_r t} + \frac{B}{10}e^{-r_2 D_r t}\right],\\
a_2 &= \frac{1}{3}p^2 + \frac{1}{3}q + \frac{1}{63}q^2 + \frac{19}{315}qp^2 + Ae^{-r_1 D_r t} + Be^{-r_2 D_r t},
\end{aligned} \tag{16}$$

where

$$\begin{aligned}
r_1 &= 2 - \frac{2}{5}q + \frac{1}{5}p^2,\\
r_2 &= 6 - \frac{2}{7}q - \frac{1}{5}p^2,
\end{aligned} \tag{17}$$

where A, B are arbitrary coefficients. If the orientational distribution is initially isotropic and a steady field is switched on at $t = 0$, Eqs. (16) lead to Benoît's low field approximation,[22] taking boundary conditions $a_1 = a_2 = 0$ at $t = 0$.

We wish to investigate the dipole moment by comparing the alignment of the rods under a steady field with alignment under an alternating field, as shown schematically in Figure 1(a). Taking boundary conditions as appropriate for these fields, we obtain from Eqs. 16:

$$\begin{aligned}
a_2^{(S)}(t_2) &= 2q(D_r t_2 - D_r^2 t_2^2) - 2p^2 D_r^2 t_2^2,\\
a_2^{(A)}(t_2) &= 2q(D_r t_2 - D_r^2 t_2^2),
\end{aligned} \tag{18}$$

where $a_2{}^{(S)}(t_2)$ and $a_2{}^{(A)}(t_2)$ are the particular solutions of $a_2(t)$ under the steady and alternating pulses respectively, evaluated at t_2, the time of the second field reversal [see Figure 1(a)]. We have expanded $a_2(t)$ to second order in t_2, taking leading orders of p and q only.

The birefringence $\Delta n(t)$ is proportional to the coefficient $a_2(t)$. Therefore, the ratio of the birefringence in the steady field Δn_S, to the birefringence in the alternating field Δn_A, at the time t_2 is given by

$$\frac{\Delta n_S(t_2)}{\Delta n_A(t_2)} = \frac{a_2^{(S)}(t_2)}{a_2^{(A)}(t_2)} = 1 + \frac{p^2}{q}D_r t_2, \tag{19}$$

or after substituting with Eqs. (15):

$$\frac{\Delta n_S(t_2)}{\Delta n_A(t_2)} = 1 + \frac{\mu(L_\tau)^2}{\Delta\alpha(L_\tau)k_B T}D_r t_2, \tag{20}$$

which is valid for p, q, and $D_r t_2$, all much smaller than 1, because it is based on lowest-order expansions in these quantities.

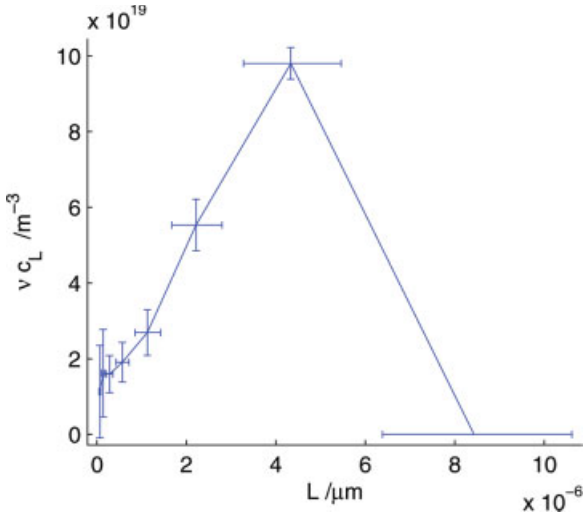

FIGURE 2 The length distribution of β-lactoglobulin fibrils in the solution, based on our previous study,[21] but with corrections made, as described in the Analysis.

The latter equation is used to estimate the dipole moment of the β-lactoglobulin fibrils as follows. In our experiment, $t_2 = 5$ ms. From the data in Figure 1(b), we measure $\Delta n_S(5\text{ ms}) = 1.4 \times 10^{-9}$, $\Delta n_A(5\text{ ms}) = 0.95 \times 10^{-9}$, and $\tau \approx 30$ ms (the time to decay by a factor of e). This time gives a rotational diffusivity $D_r = 1/(6\tau) = 5\ \text{s}^{-1}$, and a corresponding $L_\tau = 1.5\ \mu$m, again using Broersma's form of the rotational diffusivity [Eqs. (5)–(6)], where we take the fibril diameter d as 4 nm.[15,16] Using Fixman's theory [Eq. (7)], we find $\Delta\alpha(L_\tau) = 3.2 \times 10^{-30}\ \text{C m}^{-1}\ \text{V}^{-1}$ (taking the mean spacing of charges on the fibril $b = 0.45\ \mu$m and the counterion concentration $c_1 = 0.2$ mM, both as calculated in Ref. 21). With this polarizability, Eq. (20) yields $\mu(L_\tau) = 5.0 \times 10^{-25}$ C m, or 1.5×10^5 Debyes (D). (In S.I. units, 1 D $= 3.34 \times 10^{-30}$ C m).

Finding the Dipole Moment Numerically

The dipole moment can be calculated with more precision by considering the dynamics of the full polydisperse system in the electric field and calculating the system's time evolution numerically. In our previous study,[21] we determined the length distribution of the same β-lactoglobulin fibril solution by analyzing the relaxation of electric birefringence. We have found two minor errors made in the analysis of that study: we used an erroneous form of the rotational diffusivity [which is corrected in Eqs. (5)–(6)] and normalized the orientational distribution wrongly [corrected in Eq. (4)]. Having made these corrections, we obtain a length distribution, which is in fact closer to the earlier results of Ref. 21 and is shown in Figure 2, but qualitatively is unchanged.

Taking the corrected length concentrations c_L, on the array of lengths L, plotted in Figure 2, and calculating $\Delta\alpha(L)$ according to Fixman's theory[26] and $D_r(L)$ according to Broersma,[28] we can then use Benoît's model [Eqs. (1)–(4)] to predict Δn in the alternating field as a function of time. The array of lengths L contains 9 points, logarithmically sampled in the range 0.033–8.4 μm. The alignment of fibrils by the electric field is biased towards the short end of the length distribution, because of the scaling of $\Delta\alpha$ and D_r with L (see Ref. 21). The remaining unknown quantity is the dipole moment μ, which we can adjust to match calculation with measurement. A reasonable

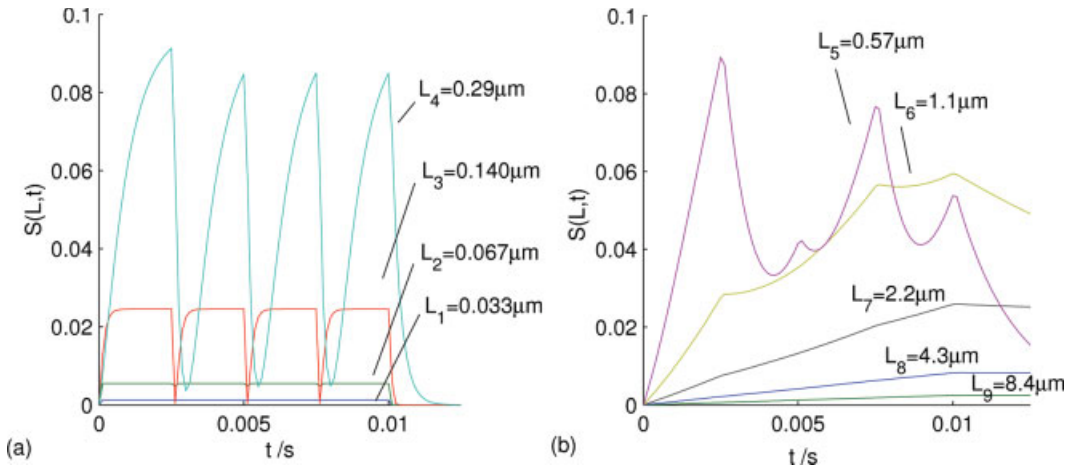

FIGURE 3 A calculation of the evolution of $S(L,t)$ for each length component in the distribution, taking $\mu' = 3.1 \times 10^{-19}$ C. The alignment is greatest for lengths around 0.29–0.57 μm. The curves are split across two graphs, (a) and (b), for easier viewing.

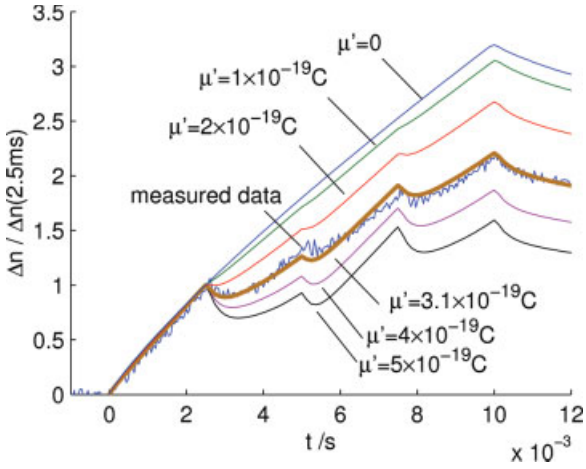

FIGURE 4 Fitting the birefringence measurement in the alternating pulse by adjusting the dipole moment (with the parameter μ', representing the dipole moment per unit length). Absolute values are ignored, by normalizing $\Delta n(t)$ by its value at $t_2 = 5$ ms. The best fit is achieved with $\mu' = 3.1 \times 10^{-19}$ C.

guess at the dependence of μ on length, would be a linear dependence:

$$\mu(L) = \mu' L, \tag{21}$$

because the fibril is a polymeric assembly of protein molecules, and any spatial inhomogeneities in the charge of the monomers must add to give the permanent dipole moment of the whole fibril.

As detailed above, we use a Runge–Kutta method to calculate the birefringence. Figure 3 shows the evolution of the alignment parameter $S(L,t)$ for each length component in the distribution, taking $\mu' = 3.1 \times 10^{-19}$ C.

In Figure 4, the measured birefringence data is compared with calculated birefringence, at a range of values of μ'. Both measured and calculated birefringence have been normalized by their values at the time of the first field reversal ($t_1 = 2.5$ ms). This normalization makes the curves diverge with increasing time, and avoids errors in the absolute value of the birefringence, thus making the curves easier to compare. The best fit is achieved taking $\mu' = 3.1 \times 10^{-19}$ C, with an error of $\pm 0.2 \times 10^{-19}$ C. (This value may be compared with the analytical estimate for μ above, which gives $\mu' = \mu(L_\tau)/L_\tau = 2.2 \times 10^{-19}$ C.) The predicted birefringence taking $\mu' = 3.1 \times 10^{-19}$ C compares very well with the measured data, even though this was the only adjustable parameter. We are therefore encouraged to think that our linear model of μ according to Eq. (21) must be approximately correct. The absolute values of measured birefringence are plotted in Figure 5, and again compared with the predicted birefringence taking $\mu' = 3.1 \times 10^{-19}$ C. There is a discrepancy of about 20% in the magnitude of the predicted birefringence, which could have been caused by errors in the calculation, especially considering the low number of length components used to describe a continuous length distribution. It could also be a shortcoming of our interpretation of the birefringence, on which we comment below.

Qualitatively, the measured birefringence signal shows that the permanent dipole moment is approximately aligned with the fibril axis. This finding is expected because the fibrils have a twisted strand structure. Because L_τ is much greater than the repeat distance of twist in the fibril, of around 26 nm,[16] any components of the permanent moment perpendicular to the fibril axis should approximately cancel. However, in order to apply Benoît's theory, we have assumed that the permanent dipole moment and fibril axis are exactly parallel. An error in this assumption would mean that our analysis represents an underestimate of the true value of the permanent electric dipole moment.[39]

DISCUSSION

Ambiguity Due to Slow Polarization

As noted earlier, it must be considered whether one or more additional components of slow polarizability of β-lactoglobulin fibrils could contribute to what we have interpreted as the permanent dipole moment. The discrepancy between the absolute magnitudes of

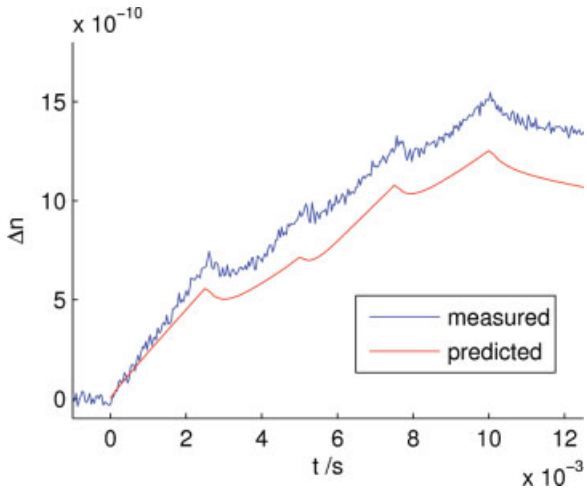

FIGURE 5 A discrepancy in absolute magnitude, of about 20%, separates the measured and predicted birefringence, taking $\mu' = 3.1 \times 10^{-19}$ C.

measured and predicted birefringence in Figure 5, taking $\mu' = 3.1 \times 10^{-19}$ C, could easily have been caused by errors in the other parameters we have used, but we cannot rule out the possibility that it is caused by a neglected slow component of the polarization. If so, our analysis represents an *apparent* permanent dipole moment, which may be an overestimate of the true permanent moment.

With further experiments, it should be possible to resolve the ambiguity. According to Benoît's model,[22] the potentials of permanent and induced dipoles in an electric field have a different dependence on the field strength E [see Eq. (2)]. Moreover, they have different relaxation times: a permanent moment can only relax by rotational diffusion, while a slow induced dipole will have some other characteristic time as well. Therefore, by studying the birefringence response to alternating pulses again, but at a range of field strengths and pulse times, it should be possible to distinguish permanent and slow dipoles unambiguously.

Dipole Moment of β-Lactoglobulin Monomers

To put the dipole moment of the fibril into context, an approximate value for the dipole moment of the native protein monomers can be calculated. Takashima et al.[40,41] and Felder et al.[24] have previously developed methods of calculating a protein's dipole moment, based on its three-dimensional (3D) structure. We follow the method of Felder et al.: taking atomic resolution 3D structures of native β-lactoglobulin deposited in the Protein Data Bank (http://www.pdb.org), partial charges are assigned to each of their atoms according to the PARSE parameter set.[42] These charges are pH dependent and are based on the charges of atoms in equivalent chemical groups in small molecules.[42] The dipole moment is calculated as the first moment of the charge distribution around the molecule's hydrodynamic center, which is estimated to be the mean of the positions of all atoms, weighted by their van der Waals radii. Bound water molecules are ignored in these calculations, but missing hydrogen atoms are constructed according to the equivalent bond lengths and angles in small molecules.[43]

The calculation was performed on β-lactoglobulin PDB structures 1BEB, 3BLG, and 1MFH, determined by X-ray crystallography, and 1CJ5, determined by NMR. (In Figure 6, 3BLG is plotted: the positions of all charged atoms, the peptide backbone, and the estimated hydrodynamic centre are shown.) For these structures, we found dipole moments of 515, 548, 538, and 475 D, respectively, at pH 3.7. The mean of these values is 519 D, which equals 1.73×0^{-27} C m in S.I. units.

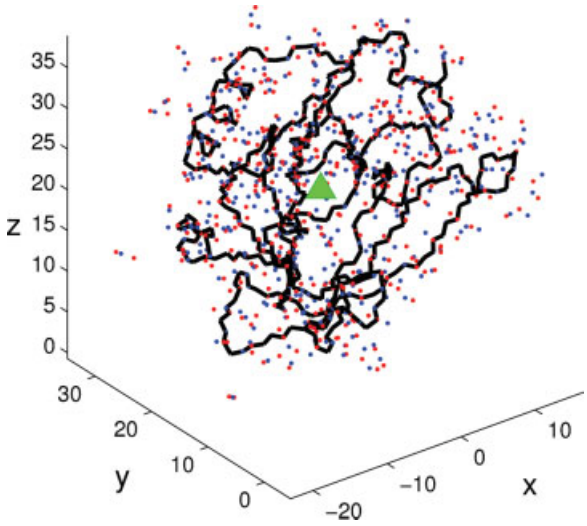

FIGURE 6 The β-lactoglobulin structure 3BLG from the Protein Data Bank (http://www.pdb.org). The positions of every (partially) charged atom, the peptide backbone, and the estimated hydrodynamic centre are shown. Key: (red) atoms with positive charge, (blue) atoms with negative charge, (–) peptide backbone, and (green) hydrodynamic center, all axes in Å.

These calculated dipole moments are reasonably close to a published measurement of the β-lactoglobulin dipole moment, of 730 D as determined by dielectric measurements[44] and mentioned in Ref. 21. However, we use our calculated values in preference to the measured value because the measured value was determined at neutral pH.

Implications for β-Lactoglobulin Fibril Structure

If we imagine a hypothetical chain of native β-lactoglobulin monomers joined "head-to-tail" to make a fibril with a line density (monomers per unit length) of 0.28 nm^{-1},[15] in such a way that their dipole moments are all pointing in the same direction as the fibril axis, we may predict a dipole moment linearly dependent on length, with $\mu'_{chain} = 1.73 \times 10^{-27}$ C m $\times$ 0.28 $nm^{-1} = 4.8 \times 10^{-19}$ C. Although this model of μ'_{chain} is crude because it is based on the approximate value of the monomer dipole moment as calculated above, and also ignores conformational changes and changes in the molecular charge density that must occur as the monomers polymerize, we have arrived at a value remarkably similar to $\mu' = 3.1 \times 10^{-19}$ C as determined by TEB above. The dipole

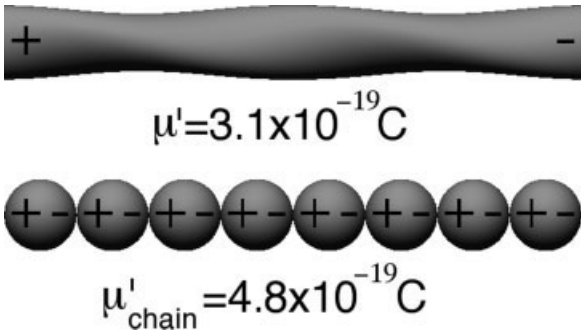

FIGURE 7 (a) The apparent permanent dipole moment per unit length of the fibril $\mu' = 3.1 \times 10^{-19}$ C, as determined from TEB, is close to (b), the approximate dipole moment of a hypothetical chain of native monomers $\mu'_{\text{chain}} = 4.8 \times 10^{-19}$ C, as calculated from their crystal structure.

moment of the fibril appears to have roughly the value we would expect, if all the monomers were ordered so that their dipoles were pointing in the same direction along the fibril axis (shown schematically in Figure 7).

Even considering the order implicit in the cross-β structural model, we might expect that the monomers in the fibril could have a disorder in the way they are joined; a cross-β structure could conceivably be formed by monomers joined in "multiple alternative registries." A permanent dipole moment would have one direct implication for the structure of the β-lactoglobulin fibrils: that the monomers in the fibril cannot be joined randomly. The measured electric birefringence contains contributions from fibrils of length up to $\sim$4 μm, i.e., of up to $\sim$1000 β-lactoglobulin molecules. With such a large number of monomers, the fibril could not have such a large dipole moment if the molecules had even a small freedom to join in either direction. Therefore, if the permanent moment we have obtained is real, it would suggest all molecules in the fibril join in a direction that is either strictly ordered or strongly biased. This direction must be such that the dipole moment of the monomer is approximately aligned with the fibril axis.

Implications for Amyloid Structure and Formation

Amyloid fibrils have some structural characteristics that are common to all and some that differ between systems. Recent NMR and X-ray diffraction studies on fibrils composed of short peptides have shown that the conformation of each peptide is highly ordered within the fibrils, as described in the Introduction. Although our result does not provide detailed information on the molecular conformation, it suggests a similar ordering of the molecules, but for fibrils based on β-lactoglobulin, a complete protein. A fibril's dipole moment may also have implications for amyloid formation. "Polar zipper" theories of amyloid fibril assembly have previously been described[6,45] where fibril assembly is driven by the electrostatic dipole–dipole interaction between the monomers or parts of the monomers. It is possible that such a mechanism could be at work in our system, and that measurements of fibril dipole moments could be used to test the polar zipper ideas.

It must be noted that the measurement of a dipole moment cannot provide any information on the cross-β motif itself—the definitive structural characteristic of amyloid fibrils. In adjacent residues along a β-strand, the polar C═O and N—H bonds of the polypeptide backbone point in opposite directions, so the backbone of the β-sheets makes no net contribution to the dipole moment of the fibril.

CONCLUSION

We have measured an apparent permanent dipole moment of β-lactoglobulin fibrils, and shown the value to be 3.1×10^{-19} C per unit length. With some additional experiments, it should be possible to refine our analysis to include the possibility of slow polarization and to obtain a more robust value for the true permanent moment, a physical property hitherto unexplored in amyloid fibril systems. The apparent dipole moment of the fibril has a magnitude similar to what we would expect if the monomers were joined head-to-tail, without changing conformation, and with their dipole moments pointing in the same direction along the fibril axis. Therefore, this result suggests an ordered joining of monomers in the fibril, which may have implications for the assembly mechanism of β-lactoglobulin fibrils in particular, and amyloid fibrils in general.

SSR would like to thank Dr. Henny Schaink for auspicious suggestions, and Fernando Perez for a perceptive insight. We gratefully acknowledge funding from the BBSRC for SSR, and the European Commission for an IHP grant awarded to the Food Physics Group of Wageningen University for a Marie Curie Training Site Fellowship (contract HPMT-2000-00188).

REFERENCES

1. Sipe, J. D. Annu Rev Biochem 1992, 61, 947–975.
2. Sunde, M.; Blake, C. C. Q Rev Biophys 1998, 31, 1–39.

3. Dobson, C. M. Phil Trans R Soc Lond B 2001, 356, 133–145.
4. Uversky, V. N.; Fink, A. L. Biochim Biophys Acta 2004, 1698, 131–153.
5. Sunde, M.; Blake, C. C. F. Adv Protein Chem 1997, 50, 123–159.
6. Tycko, R. Curr Opin Struct Biol 2004, 14, 96–103.
7. Nilsson, M. R. Methods 2004, 34, 151–160.
8. Jaroniec, C. P.; MacPhee, C. E.; Astrof, N. S.; Dobson, C. M.; Griffin, R. G. Proc Natl Acad Sci USA 2002, 99, 16748–16753.
9. Jaroniec, C. P.; MacPhee, C. E.; Bajaj, V. S.; McMahon, M. T.; Dobson, C. M.; Griffin, R. G. Proc Natl Acad Sci USA 2004, 101, 711–716.
10. Petkova, A. T.; Ishii, Y.; Balbach, J. J.; Antzutkin, O. N.; Leapman, R. D.; Delaglio, F.; Tycko, R. Proc Natl Acad Sci USA 2002, 99, 16742–16747.
11. Nelson, R.; Sawaya, M. R.; Balbirnie, M.; Madsen, A. O.; Riekel, C.; Grothe, R.; Eisenberg, D. Nature 2005, 435, 773–778.
12. Dobson, C. M. Semin Cell Dev Biol 2004, 15, 3–16.
13. Bromley, E. H. C.; Krebs, M. R. H.; Donald, A. M. Faraday Discuss 2005, 128, 13–27.
14. Gosal, W. S.; Clark, A. H.; Ross-Murphy, S. B. Biomacromolecules 2004, 5, 2408–2419.
15. Aymard, P.; Nicolai, T.; Durrand, D. Macromolecules 1999, 32, 2542.
16. Arnaudov, L. N.; de Vries, R.; Ippel, H.; van Mierlo, C. P. M. Biomacromolecules 2003, 4, 1614.
17. Sagis, L. M. C.; Veerman, C.; van der Linden, E. Langmuir 2004, 20, 924–927.
18. Gosal, W. S.; Clark, A. H.; Pudney, P. D. A.; Ross-Murphy, S. B. Langmuir 2002, 18, 7174.
19. Cannan, R. K.; Palmer, A. H.; Kibrick, A. C. J Biol Chem 1941, 142, 803.
20. Rogers, S. S.; Venema, P.; Sagis, L. M. C.; van der Linden, E.; Donald, A. M. Macromolecules 2005, 38, 2948–2958.
21. Rogers, S. S.; Venema, P.; van der Ploeg, J.; Sagis, L. M. C.; Donald, A. M.; van der Linden, E. Eur Phys J E 2005, 18, 207–217.
22. Benoît, H. Ann Phys 1951, 6, 561.
23. O'Konski, C. T.; Zimm, B. H. Science 1950, 111, 113–116.
24. Felder, C. E.; Botti, S. A.; Lifson, L.; Silman, I.; Sussman, J. L. J Mol Graph Model 1997, 15, 318.
25. Hagerman, P. J. Curr Opin Struct Biol 1996, 6, 643–649.
26. Fixman, M. Macromolecules 1980, 13, 711–716.
27. Riseman, J.; Kirkwood, J. G. J Chem Phys 1950, 18, 512–516.
28. Broersma, S. J Chem Phys 1960, 32, 1626–1631.
29. Tirado, M. M.; de la Torre G. J Chem Phys 1980, 73, 1986–1993.
30. Elias, J. G.; Eden, D. Macromolecules 1981, 14, 410–419.
31. Manning, G. S. Biophys Chem 1978, 9, 65–70.
32. Mandel, M.; Odijk, T. Annu Rev Phys Chem 1984, 35, 75.
33. Manning, G. S. J Chem Phys 1989, 90, 5704–5710.
34. Holm, C.; Rehahn, M.; Oppermann, W.; Ballauff, M. Adv Polym Sci 2004, 166, 1.
35. Tricot, M.; Houssier, C. Macromolecules 1982, 15, 854–865.
36. van Dijk, W.; van der Touw, F.; Mandel, M. Macromolecules 1981, 14, 792–795.
37. Bordi, F.; Cametti, C.; Colby, R. H. J Phys: Condensed Matter 2004, 16, R1423–R1463.
38. Fuller, G. G. Optical Rheometry of Complex Fluids; Oxford University Press: New York, 1995.
39. Thurston, G. B.; Bowling, D. L. J. Colloid Interface Sci 1969, 30, 34–45.
40. Takashima, S. Biopolymers 2001, 58, 398–409.
41. Takashima, S.; Yamaoka, K. Biophys Chem 1999, 80, 153–163.
42. Sitkoff, D.; Sharp, K. A.; Honig, B. J Phys Chem 1994, 98, 1978–1988.
43. Sutton, L. E., Ed. Tables of Interatomic Distances and Configuration in Molecules and Ions; The Chemical Society: London; Special Publication 11 (1958) and 18 (1965).
44. Ferry, J. D.; Oncley, J. L. J Am Chem Soc 1941, 63, 272.
45. Perutz, M. F.; Johnson, T.; Suzuki, M.; Finch, J. T. Proc Natl Acad Sci USA 1994, 91, 5355–5358.

Reviewing Editor: Nancy Stellwagen